STScI | SPACE TELESCOPE SCIENCE INSTITUTE

Instrument Science Report ACS 2023-01

Corrections to Commanding Overheads for ACS/WFC Exposures

J. E. Ryon & N. A. Grogin

February 20, 2023

Abstract

In this report, we study corrections to the commanding overheads of ACS/WFC exposures. Commanding overheads are time delays associated with operating the instrument, which should be included in the DARKTIME keyword value. Previous work determined that corrections to the commanding overheads (as well as DARKTIME) on the order of a few seconds was necessary. We revisit these corrections in light of the fading trends of hot pixel dark rates discussed in Ryon et al. (2022), and utilize the fading trends themselves to determine that no commanding overhead corrections are required for the four ACS/WFC observing modes (full-frame/subarray and unflashed/post-flashed). We have updated the WFC CCDTABs to reflect this result.

1 Introduction

To take an exposure with the Advanced Camera for Surveys (ACS) Wide Field Channel (WFC), a series of commands operate the instrument hardware. Time delays associated with executing these commands are called commanding overheads. Dark current accrues the entire time WFC is in ACCUM mode[1], which includes certain commanding overheads. Accurate knowledge of the overheads for different observing modes is therefore essential to properly subtract dark current from science data, especially for CCD hot pixels (>0.14 e^-/s).

[1] `https://hst-docs.stsci.edu/display/ACSIHB/7.3+Operating+Modes`

The overheads also come into play when using hot pixels for other means, for instance, determining the parameters of the pixel-based charge transfer efficiency (CTE) model (Anderson & Ryon, 2018).

The DARKTIME header keyword found in WFC data is meant to reflect the total amount of time in seconds that dark current accumulates during a given exposure, including commanding overheads. The DARKTIME value is calculated from the timings in *HST* telemetry associated with each exposure, and is given by

$$\mathrm{DARKTIME} = \mathrm{EXPTIME} + \mathrm{FLASHDUR} + t_{\mathrm{theo}}, \tag{1}$$

where header keywords EXPTIME and FLASHDUR are the exposure time and LED post-flash duration, respectively, and t_{theo} is the theoretical commanding overhead, all in units of seconds. For post-flashed exposures, $t_{\mathrm{theo}} \approx 6$s, while for unflashed exposures, $t_{\mathrm{theo}} \approx 3$s. There are variations up to a few tenths of a second between identically-commanded exposures.

Empirical estimates of the commanding overheads have been made by measuring the total dark signal in stable, hot pixels in dark exposures (N. Miles priv. comm.). In bias-, CTE-, and post-flash-corrected dark frames, the signal S in e^- of an individual pixel is given by

$$S = d \times (\mathrm{EXPTIME} + \mathrm{FLASHDUR} + t_{\mathrm{emp}}), \tag{2}$$

where d is the dark rate of the pixel in e^-/s and t_{emp} is the empirical commanding overhead in seconds. Assuming d is provided in the superdark (dark reference file) for a given anneal period, then by finding S in a number of individual frames for a large sample of pixels, the best value of t_{emp} can be calculated. Superdarks are created by differencing stacks of long (1000.5s) and short (0.5s) post-flashed dark frames, which should remove any dependence of d on commanding overheads.

If the DARKTIME keyword correctly includes all commanding overheads, then we would expect that $t_{\mathrm{theo}} = t_{\mathrm{emp}}$. Previous work found small discrepancies, $\Delta t = t_{\mathrm{emp}} - t_{\mathrm{theo}} > 0$, for all four categories of WFC observing modes: full-frame and subarray, both unflashed and post-flashed (N. Miles priv. comm.). The discrepancies determined by that work, which are essentially corrections to the DARKTIME keyword, are listed in Table 1 and in the CCD calibration parameter table (CCDTAB). The calibration pipeline CALACS, as of version 10.3.3, adds the Δt value appropriate for the observing mode to the input image's DARKTIME keyword during the initial processing task ACSCCD. The superdark is then scaled by the corrected DARKTIME value and subtracted from the input image during the dark correction step DARKCORR[2] (Lucas et al., 2022).

Ryon et al. (2022), hereafter R22, have recently shown that the dark rate of many stable, hot pixels decreases steadily as a function of exposure time. This affects measurements of t_{emp} from these hot pixels and calls into question the validity of Δt in Table 1. A second look into the corrections to commanding overheads is therefore warranted. In Section 2, we briefly discuss two initial approaches to measuring commanding overheads that take into account fading dark rates. Then in Sections 3 and 4, we describe a novel approach to determining commanding overheads and its application to full-frame and subarray data, respectively. Finally, we summarize our results and conclude in Section 5.

[2] `https://github.com/spacetelescope/hstcal/releases/tag/2.7.2`

Table 1: Original Corrections to DARKTIME, Δt, in seconds

	Full-Frame	**Subarray**
Unflashed	0.21	2.45
Post-Flashed	2.43	4.46[a]

[a] Computed rather than measured. The difference between the full-frame post-flashed and unflashed modes was added to the unflashed subarray Δt value. Assumes post-flashing takes the same amount of additional commanding time, no matter the detector readout mode.

2 Initial Analysis Attempts

Our initial attempts to measure the empirical commanding overheads utilized similar techniques to those described in Section 1. The key difference was to account for the decrease in dark rate with DARKTIME, or the fading trends, of very hot pixels (>5 e^-/s) as described in R22. In both approaches, individual bias-, CTE-, and post-flash-corrected dark frames from various anneal periods over the lifetime of ACS provided the hot pixel signals S. Full-frame and subarray data were analyzed.

In the first approach, we adjusted the dark rate d of very hot pixels in the superdark to the appropriate value for each individual frame's DARKTIME, based on the second-degree polynomial fit to the pixel's dark rate as a function of DARKTIME from R22. Our second approach was to select hot pixels that did not fade significantly over 1000s of exposure time, meaning d could simply be taken from the superdark.

Values of Δt for both approaches were calculated using Eq 2, and were found to disagree by several seconds. Analysis of data from many anneal periods and hot pixels selected via different criteria gave inconsistent results as well. Additionally, we discovered ensemble frame-to-frame variation of hot pixel signal that further complicated the analysis, and will be described more fully in a future report. Neither approach reproduced the results from Table 1 (though this was not necessarily expected). In addition, because the superdark for a given anneal period is created by stacking post-flashed, full-frame darks, the analysis was somewhat circular for that particular observing mode.

3 Full-frame Data

During the initial analysis, we noted that plots of hot pixel dark rate as a function of DARKTIME in individual full-frame images (Figures 3 and 4 in R22) showed sharp turnovers at short DARKTIME when $\Delta t > 0$s. As in R22, dark rate is the number of electrons in the hot pixel divided by the DARKTIME of the frame. In Figure 1, we recreate Figure 3 from R22 for all unflashed (circles) and post-flashed (plus signs) full-frame data from the October 2020 anneal period. This plot shows an example hot pixel located near the amplifier in amp C at (570, 174). The dark rates are calculated after applying three different sets of Δt values to DARKTIME: zero seconds for both unflashed and post-flashed frames (blue markers), five seconds for both (green markers), and the values listed in Table 1, 0.21s for unflashed frames and 2.43s for post-flashed frames (orange markers). (Five seconds was arbitrarily chosen as

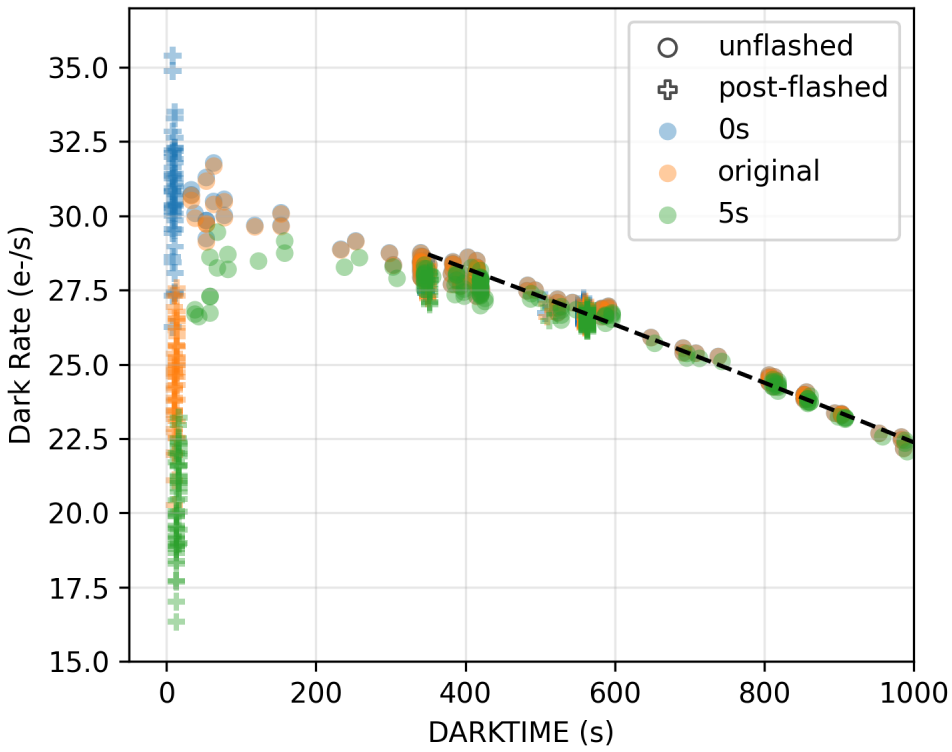

Figure 1: Dark rate as a function of DARKTIME for example pixel (570, 174) in amp C from every dark and external full-frame image in the Oct 2020 anneal period. Unflashed frames are plotted with circles and post-flashed with plus signs. The value of Δt applied to DARKTIME is represented by the color of the data points. The original values are 0.21s for unflashed frames and 2.43s for post-flashed frames. The dashed black line shows a quadratic fit to the $\Delta t = 0$s data with 350s<DARKTIME<2000s from R22.

a large example value for Δt.)

Figure 1 demonstrates clearly that as Δt increases, the turnover at short DARKTIME in the fading trend of this hot pixel becomes sharper. As discussed in R22, the large scatter at short DARKTIMEs is expected and due to dark current noise, post-flash noise, readnoise, and the pixel-based CTE correction. Even with this large scatter, it is clear that when $\Delta t = 0$s, the dark rates for short DARKTIMEs align best with the overall fading trend.

We posit that a smoothly-varying fading trend is expected for hot pixels. In other words, there is no physical reason for hot pixels to brighten dramatically over the first 50 to 100 seconds of an exposure. However, poor CTE correction of hot pixels in external frames with short DARKTIMEs (and therefore low backgrounds) could cause them to appear to have low dark rates. CTE losses are strongly tied to distance from the readout amplifier, so this effect should be minimal near to the amplifier.

Therefore, we define a new approach: find values of Δt that result in the least difference between observed and expected dark rates in hot pixels near the readout amplifiers at short DARKTIMEs. To do this, we again utilize the hot pixel dark rates and polynomial fits to fading trends from R22. Separately for post-flashed and unflashed full-frames, the median observed dark rate of each hot pixel in images with DARKTIME < 100s is found. We also calculate the median DARKTIME of these images and find the expected dark rate at those

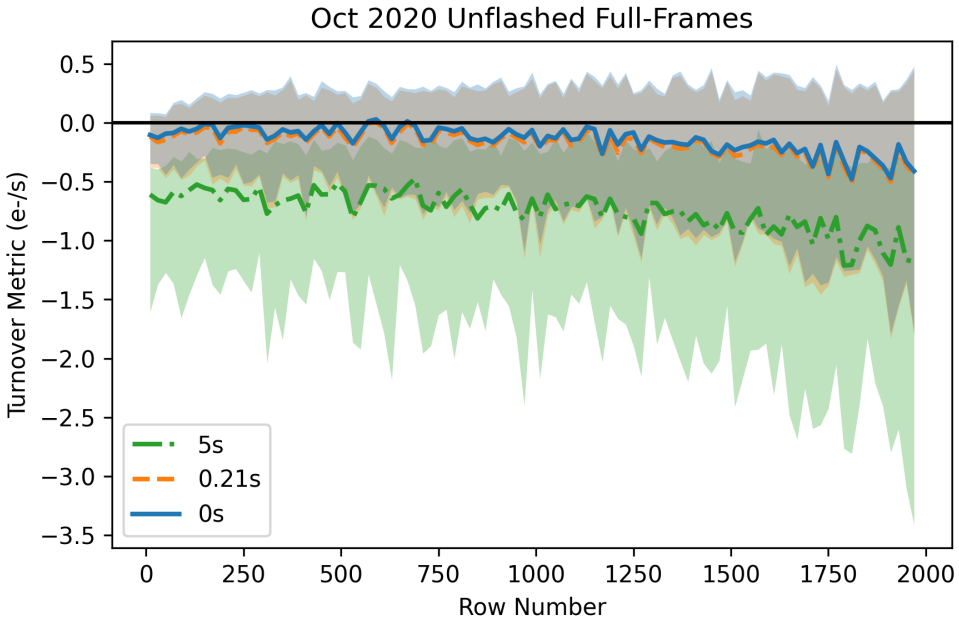

Figure 2: Turnover metric, or the difference between observed and expected dark rates in unflashed full-frame images with DARKTIME < 100s, as a function of row number. The solid lines represent the median turnover metric while the shaded regions show the 1σ scatter. The colors correspond to three values of Δt. The original Δt is shown in orange. The black line highlights a turnover metric of zero, which is the desired value for low row number.

median DARKTIMEs from the 2nd-degree polynomial fits to the hot pixel fading trends. We call the difference between the median observed dark rate and expected dark rate the turnover metric. When the turnover metric is zero, the expected and observed dark rates agree, meaning there is little to no turnover in the fading trend at short DARKTIMEs. When it is negative, the observed dark rates are below expectations and when positive, they are above expectations.

In Figure 2, we plot the turnover metric as a function of row number for unflashed full-frame data from the Oct 2020 anneal period. The solid lines represent the median turnover metric in bins of 20 rows, and the shaded regions represent 1σ scatter in the turnover metric. The colors correspond to three values of Δt: 0s (blue), 0.21s (orange), and 5s (green). Figure 3 is the same as Figure 2 but for post-flashed full-frame data.

All three median turnover metric lines in Figure 2 largely fall below zero, but tend towards zero nearer to the readout amplifier (lower row number). CTE losses likely drive the decreasing turnover metrics as row number increases. We expect poor CTE correction of hot pixels in frames with short DARKTIMEs and low backgrounds, and this effect becomes stronger further from the amplifier. The blue $\Delta t = 0$s line is slightly closer to zero than the orange line (original Δt), whereas the green $\Delta t = 5$s line is far below both. This suggests that $\Delta t = 0$s results in the smoothest fading trends for hot pixels where CTE losses are least likely to contribute. In other words, the DARKTIME keyword for unflashed full-frame data requires no correction for additional commanding overhead.

In Figure 3, the median turnover metrics increase with distance from the readout ampli-

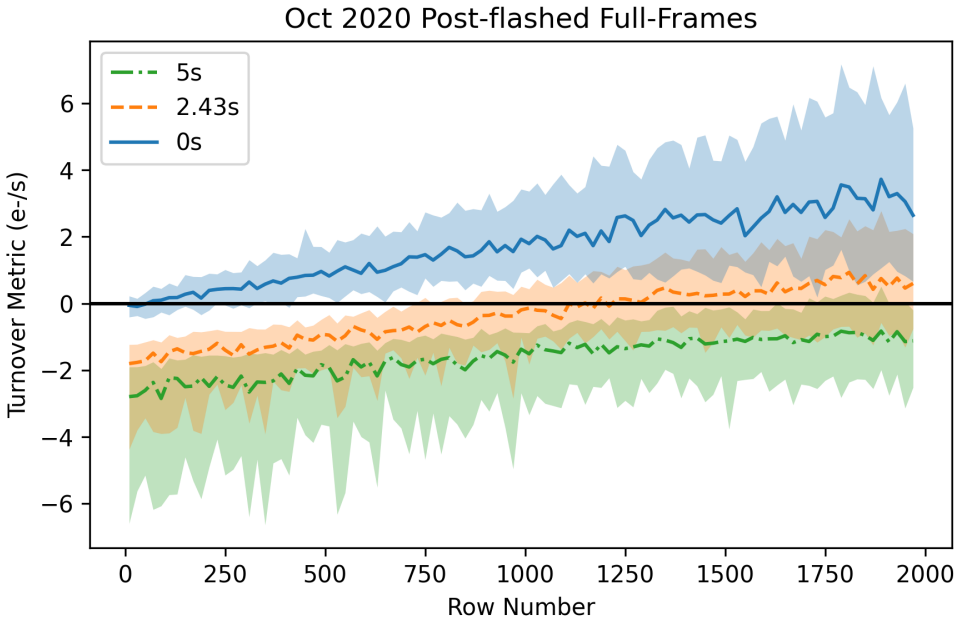

Figure 3: Same as Figure 2 but for post-flashed full-frame images.

fier, in contrast to Figure 2. While it is not entirely clear why this increases occurs, we know hot pixels in post-flashed images should not suffer from poorly-corrected CTE losses due to the relatively high background (median 55 e^-). We suggest Figure 3 actually shows that the pixel-based CTE correction is slightly overcorrecting hot pixels far from the amplifier, which gives rise to the upward trends with increasing row number. However, at low row number, where any CTE effects should be minimized and turnover metrics are therefore most reliable, we find that the blue $\Delta t = 0$s results in a turnover metric of zero. The two lines with positive values of Δt fall far below zero turnover metric at low row number. Therefore, as for unflashed frames, there is no additional commanding overhead needed for post-flashed full-frame data.

To confirm these results, we analyzed full-frame data from two additional anneal periods in the same way: Dec 2021 and Jan 2011. The former was chosen because a calibration program to obtain subarray data for this purpose was executed during this anneal, and will be discussed in Section 4. The latter occurred before post-flashing was supported and CTE losses were significantly less than they are now. Figure 4 contains the same plots as Figures 2 and 3 for these two anneals. We find essentially the same results as for the Oct 2020 anneal. The Dec 2021 plots clearly show the turnover metric reaching zero at low row number for both unflashed and post-flashed full-frames. In the Jan 2011 plot, the turnover metric lines are nearly flat at zero as a function of row number, suggesting CTE losses are minor (or the pixel-based CTE correction is more effective) at this early date.

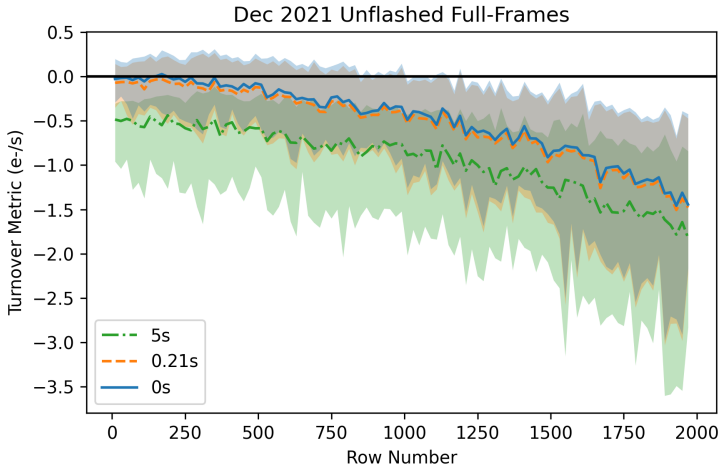

(a)

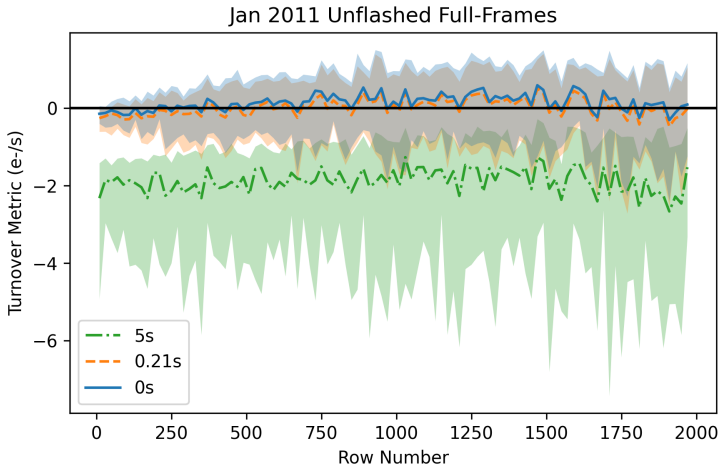

(b)

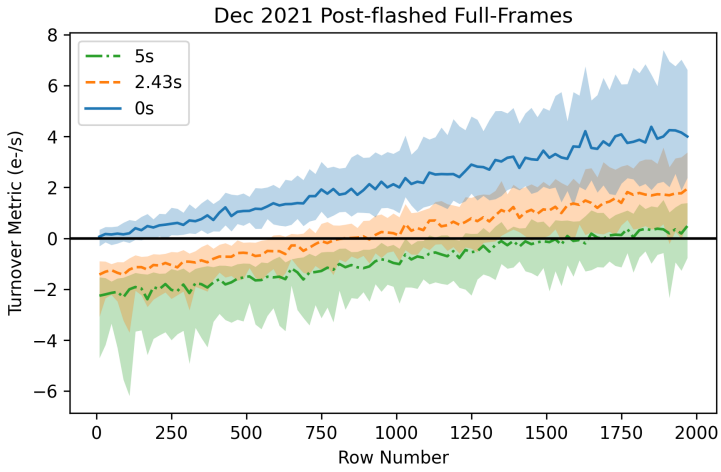

(c)

Figure 4: Same as Figures 2 and 3 but for the Dec 2021 (unflashed and post-flashed full-frames) and Jan 2011 (unflashed full-frames only) anneal periods.

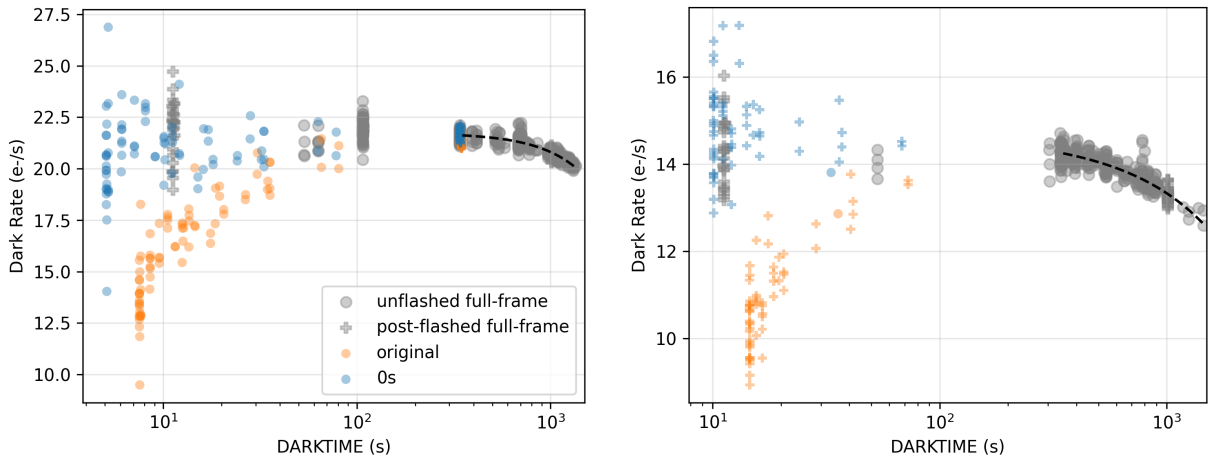

(a) Pixel (3662, 1950) in amp B from the Dec 2021 anneal period.

(b) Pixel (2721, 2047) in amp B from the Oct 2018 anneal period.

Figure 5: Dark rate as a function of DARKTIME for two example pixels. Unflashed frames are plotted with circles and post-flashed with plus signs. For the subarray data, the value of Δt applied to DARKTIME is represented by the color of the data points. The 'original' values are 2.45s for unflashed frames and 4.46s for post-flashed subarrays. Full-frame data are gray markers. The dashed black line shows a quadratic fit to the $\Delta t = 0$s full-frame data with 350s<DARKTIME<2000s from R22.

4 Subarray Data

A number of subarray images were taken during the Oct 2018 and Dec 2021 anneals, almost entirely for flux calibration programs (15526, 15529, 16514, & 16530). Another Dec 2021 calibration program, 16893, obtained 337-second unflashed and post-flashed subarray darks, which were included in the (ultimately unsuccessful) approaches described in Section 2. Nearly all of the data from Oct 2018 is post-flashed, whereas most of the data from Dec 2021 is unflashed.

In Figure 5, we plot dark rate as a function of DARKTIME for example hot pixels in unflashed (circles) and post-flashed (plus signs) data from the Oct 2018 and Dec 2021 anneal periods. The chosen pixels are located close to amplifier B in both anneals. We plot subarray data with two sets of Δt values added to DARKTIME: zero seconds (blue markers) and the values listed in Table 1, 2.45s for unflashed frames and 4.46s for post-flashed frames (orange markers). Because all of the subarray data have DARKTIME $\lesssim$ 340s, we also plot full-frame dark rates ($\Delta t = 0$s, gray markers) and the 2nd-degree polynomial fit to show the overall fading trend for these pixels. The x-axis is plotted in log scale in order to highlight the behavior of dark rates at very short DARKTIME.

Figure 5 demonstrates that the subarray data with $\Delta t = 0$s align closely with the full-frame dark rates and the overall fading trend for both hot pixels. In contrast, the data with original Δt values turn over strongly at short DARKTIME for both post-flashed and unflashed data. Dark rates in the post-flashed subarray data at DARKTIME $\sim$ 340s agree well with the full frame data at similar DARKTIME.

Similarly to the full-frame data, we calculate turnover metrics for the hot pixels in the subarray data. The median observed dark rate of each hot pixel in subarray images with

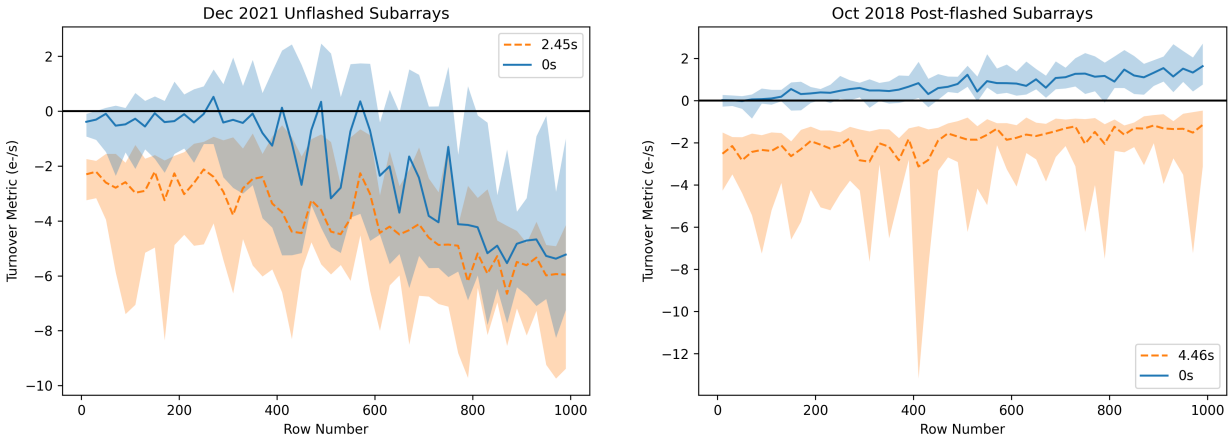

(a) Unflashed subarray data from the Dec 2021 anneal period.

(b) Post-flashed subarray data from the Oct 2018 anneal period

Figure 6: Same as Figure 2 but for subarray data and two values of Δt. The original Δt is shown in orange, and $\Delta t = 0$s is shown in blue.

DARKTIME $<$ 15s (22s) for unflashed (post-flashed) data is found. We also calculate the median DARKTIME of these images and find the expected dark rate at those median DARKTIMEs from the 2nd-degree polynomial fits to the hot pixel fading trends in the full-frame data.

We plot the turnover metric as a function of row number for subarray data from the Dec 2021 and Oct 2018 anneal periods in Figure 6. Again, the solid lines represent the median turnover metric in bins of 20 rows, and the shaded regions represent 1σ scatter in the turnover metric. The colors correspond to Δt values: blue represents 0s for both datasets, whereas orange represents 2.45s for unflashed data and 4.46s for post-flashed data. Despite the increased scatter, the turnover metric lines in Figure 6 behave similarly to those for full-frame data. No additional commanding overheads are needed to produce smooth fading trends for either unflashed or post-flashed subarray data.

5 Conclusions

In this study, we revisited the commanding overheads of ACS/WFC exposures, including full-frame and subarray images, both post-flashed and unflashed. We utilized knowledge of fading hot pixels from R22 to develop a new approach to measuring the commanding overhead corrections Δt. This new approach involved comparing observed and expected dark rates of very hot pixels ($>5e^-/s$) at short DARKTIME, and found that all observing modes require approximately zero seconds of correction to commanding overheads ($\Delta t \approx 0$s).

Only post-SM4 full-frame data and subarrays from Cycle 24 and later were included in the initial study of commanding overheads (N. Miles priv. comm.). We have updated the OVRHFLS and OVRHUFLS columns in the WFC CCDTABs to zero seconds and delivered them to the Calibration Reference Data System (CRDS). Affected data will be reprocessed shortly after the publication of this report. This will reduce DARKTIMEs and remove any residual dark current, which is typically a minor affect, in those data.

Acknowledgements

The authors thank the following ACS team members for their helpful comments: Nimish Hathi, Meaghan McDonald, David Stark, Roberto Avila, and Yotam Cohen.

This work makes use of `jupyter` (Kluyver et al., 2016), `numpy` and `scipy` (Virtanen et al., 2019), `pandas` (McKinney, 2010), `astropy` (Astropy Collaboration et al., 2013; Price-Whelan et al., 2018), and `matplotlib` (Hunter, 2007).

References

Anderson, J., & Ryon, J. E. 2018, Improving the Pixel-Based CTE-correction Model for ACS/WFC, ACS ISR 2018-04, STScI

Astropy Collaboration, Robitaille, T. P., Tollerud, E. J., et al. 2013, A&A, 558, A33

Hunter, J. D. 2007, Computing in Science & Engineering, 9, 90

Kluyver, T., Ragan-Kelley, B., Pérez, F., et al. 2016, in Positioning and Power in Academic Publishing: Players, Agents and Agendas, ed. F. Loizides & B. Schmidt, IOS Press, 87 – 90

Lucas, R. A. et al. 2022, ACS Data Handbook, Version 11.0 (Baltimore: STScI)

McKinney, W. 2010, in Proceedings of the 9th Python in Science Conference, ed. S. van der Walt & J. Millman, 51 – 56

Price-Whelan, A. M., Sipőcz, B. M., Günther, H. M., et al. 2018, AJ, 156, 123

Ryon, J. E., Grogin, N. A., & McDonald, M. C. 2022, Fading Hot Pixels in ACS/WFC, ACS ISR 2022-07, STScI

Virtanen, P., Gommers, R., Oliphant, T. E., et al. 2019, arXiv e-prints, arXiv:1907.10121